The Effect of Airframe Flexibility on Dynamic Landing Gear Loads

Terrin Stachiw*, Fidel Khouli†, Robert G. Langlois‡, Fred Afagh§
Carleton University, Ottawa, Ontario, K1S 5B6

Advancements in simulation and analysis tools and the use of composite materials have allowed for optimized and lightweight aircraft structures; however, that comes at a cost of increased airframe flexibility. The importance of including airframe flexibility effects in landing loads analysis was recognized in the 1950s where these effects resulted in either an increase or decrease in loads transferred to the airframe. Since that time, there have been significant developments in substructure coupling methods for dynamic analysis allowing for accurate and computationally-efficient analysis of coupled substructure loads. Despite this, common practice is to obtain landing loads by representing the airframe as a rigid structure, then apply this loading to a dynamic finite element simulation. This simplification of the airframe is also manifested in the standard landing gear drop-test technique where a landing gear is attached to a rigid structure that represents the aircraft. In this study, the structural dynamics for a generic 150 passenger regional jet in three landing conditions were compared when using a flexible and fully-rigid airframe model. In general, the peak forces were decreased but the peak moments were increased at the attachment point of the main landing gear for a fully-flexible airframe model when compared to the rigid equivalent. The inclusion of flexibility effects also resulted in the introduction of higher-frequency vibrations and a change in the open-loop response of the aircraft.

I. Nomenclature

C_0	=	Hydraulic damping coefficient
F_0	=	Air-spring pre-load force
F_d	=	Hydraulic damping force
F_s	=	Air-spring force
I	=	Second moment of area
s	=	Landing gear stroke distance
$\dot{s}$	=	Time derivative of landing gear stroke distance; stroke velocity
x	=	Aircraft body axis fore/aft direction; positive forward
y	=	Aircraft body axis left/right direction; positive starboard
z	=	Aircraft body axis up/down direction; positive down
η	=	Non-dimensional position along the wing with 0 at the wing root and 1 at the wing tip
γ	=	Heat capacity ratio
θ	=	Pitch angle
ϕ	=	Roll angle
ψ	=	Yaw angle

II. Introduction

Landing is a critical phase in aircraft operation in which most accidents tend to occur. Accurate prediction of aircraft dynamic landing loads is crucial for stressing and designing the airframe. Traditionally, the dynamic forces

*M.A.Sc. Candidate, Mechanical and Aerospace Engineering, Carleton University, Ottawa, Ontario.
†Assistant Professor, Mechanical and Aerospace Engineering, Carleton University, Ottawa, Ontario.
‡Professor, Mechanical and Aerospace Engineering, Carleton University, Ottawa, Ontario.
§Professor, Mechanical and Aerospace Engineering, Carleton University, Ottawa, Ontario.

and moments experienced by the landing gear (LG) during the landing phase that are used to stress the airframe are developed by representing the aircraft as a rigid structure. This assumption is manifested in a LG drop test where the LG is attached to a structure that represents the aircraft as a rigid mass. With the advent of highly-optimized structures and composite materials, aircraft are becoming lighter than ever and this comes at the cost of increased structural compliance. It is hypothesized that this structural deformation alters the peak loads experienced by the structure and the loading regime under which the aircraft responds.

The importance of including airframe flexibility was investigated in 1956 by Cook and Milwitzky, who found that the interactions with the flexible structure and dynamic magnification effects could either reduce or increase the loads when compared to a completely rigid airframe [1]. In this investigation, the aircraft structural flexibility was reduced to an equivalent spring-mass-damper system and, as such, cannot capture higher-frequency modes. Reviews of landing dynamics conducted by Krüger et al. [2] and by Pritchard [3] indicate the importance of including aircraft flexibility effects in the modelling of ground dynamics for simulation. The work by Pritchard focuses on the importance of airframe flexibility in predicting and managing gear instabilities, such as shimmy; and the work by Krüger covers the requirements for the simulation of various cases, including the shimmy problem, and the dynamics at touchdown and ground-roll.

Brutto et al. [4] and Kaphane [5] used a reduced finite element model (FEM) of the airframe, which reduces the major aircraft components to equivalent bar elements and is commonly referred to as a *stick model*. These authors used their stick models to perform landing and other ground dynamic simulations. For early aircraft development where detailed geometry and other features may not be known, Krüger [6] used a reduced model made up of concentrated mass elements connected by torsional springs to capture only the bending of the structure, and used this model to compare to the loads developed during landing simulations when using a rigid airframe model. Kaphane [7] extended their model to include a flexible LG model that represents the struts as beam elements. Nguyen et al. [8] and Leo et al. [9] both used a rigid aircraft model and represented the LG as a flexible structure for landing simulations of a fixed LG design.

Sartor et al. [10] and Lee et al. [11] both used a rigid representation of the aircraft to develop landing loads during hard landing cases, then Lee at al. applied these loads to a FEM to evaluate the stresses in the detailed representation of the stuctural components. Recent investigation by Bronstein et al. [12], and Cumnuantip and Krüger [13] have used a stick model to develop dynamic landing loads, which were subsequently applied to a full FEM for transient analysis. Cumnuantip and Krüger also investigated the effects of the number of included modes on predicted loads, and the effect of the topology used to attach the LG to the FEM.

A flowchart of the methodology for the work in the present study is given in Fig. 1. Section III presents the development of the stick model in *NASTRAN* that is based on literature without the need of a full FEM representation. The *MSC Adams* simulation model and set-up are described in Section IV. The effect of flexibility of various parts of the model is investigated in order to determine the minimum representation of airframe flexibility required for dynamic loads analysis. Results are provided and discussed in Section V with conclusions made in Section VI.

III. Development of the Stick Model

A. Aircraft Model

The aircraft used in this study is a generic regional jet with a capacity of 150 passengers. It has cantilevered shock-strut type LG in a tricycle configuration. Similar aircraft include the Boeing 737, Airbus A319, Airbus A220, and Embraer E-195. This class was chosen as it is among the most common in commercial operation and, as such, there is ample reference literature surrounding it. For reference, the aircraft has a span of 115 ft [35 m], a length of 130 ft [40 m], an operating empty weight (OEW) of 80 000 lbs [36 360 kg], and a maximum takeoff weight (MTOW) of 150 000 lbs [68 180 kg].

B. Stick Model

It is common industrial practice to begin with a full FEM of an aircraft then reduce it to an equivalent model using various dynamic reduction techniques or by the development of an equivalent stick model using unitary loads, as introduced by Elsayed et al. [14]. The reduced model represents the elastic axis of the wings, fuselage, and vertical and horizontal stabilizers as bar elements (CBAR in *NASTRAN*). Ideally, these bar elements retain the same bulk stiffness properties such that they are statically equivalent and the stiffness and mass distributions allow for equivalent natural mode shapes and frequencies such that they are dynamically equivalent.

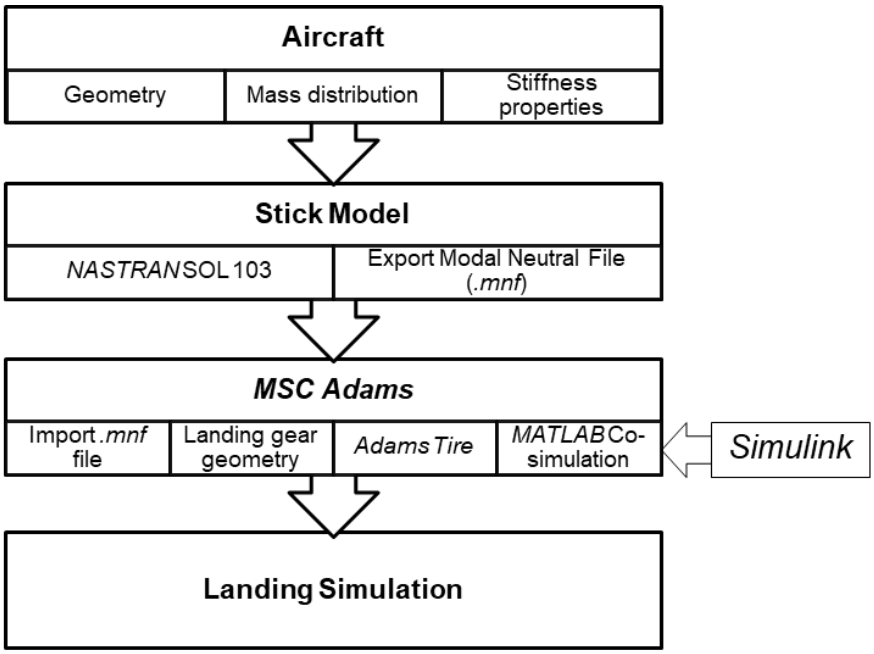

Fig. 1 Flowchart outlining methodology for the analysis.

In the present investigation, a full FEM was not available so a stick model was developed directly from the aircraft geometry. The mass and stiffness distributions were developed from typical values available in literature and then were tuned in order to match natural frequencies of similar aircraft also available in literature. The major elements of the stick model are shown in Fig. 2a. In order to allow for better visualization of the structural dynamics, especially for torsional modes, plotting elements (PLOTEL in *NASTRAN*) were used. The full stick model used for dynamic analyses is shown in Fig. 2b.

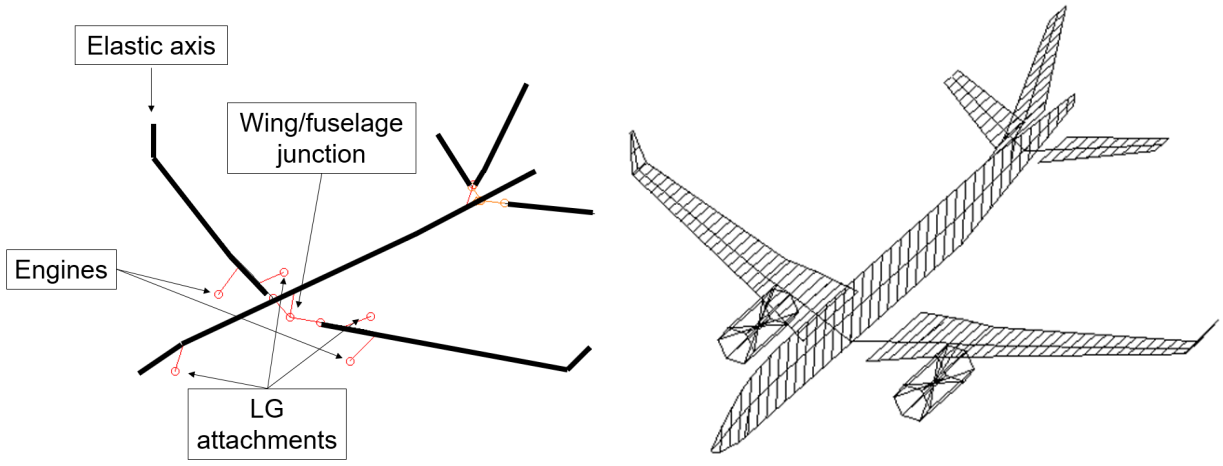

(a) Annotated stick model. **(b) Final stick model with plotting elements.**

Fig. 2 Stick model used in dynamic analyses.

C. Mass Distribution

All simulations were performed using the OEW configuration in this investigation. The OEW configuration is the low boundary of the aircraft weight envelope and represents the structural mass of the aircraft plus any fluids required for

operation. It does not include any fuel beyond the unusable or trapped fuel. Roskam [15] provides empirical methods for estimating the weight of aircraft components (i.e. wings, fuselage, empennage, LG) as a function of the aircraft total weight; the mass of the components were estimated using this method.

The distribution of mass along the length of the components was required such that concentrated mass elements (CONM2 in *NASTRAN*) can be assigned to each node with their corresponding mass, inertias, and offsets. For the wings and the empennage, the mass at node i is the ratio of the projected area of the wing section to the total projected area of the wing multiplied by the total wing mass. One section shall begin halfway between the current node and the preceding node, and end halfway between the current node and the following node. Similarly for the fuselage, the equivalent concentrated mass element was calculated as the ratio of the volume of the fuselage section to the total fuselage volume multiplied by the total fuselage mass.

The engines were modelled as concentrated mass elements with corresponding inertias that are rigidly attached to the wings. The mass was taken to be that of a representative engine and the moments of inertia were calculated as the inertia of a uniform cylinder with equivalent dimensions to those of a representative engine.

D. Stiffness Distribution

Various sources give example distributions of the cross-sectional properties, such as the second moments of area, of reference wings, fuselages and empennages [6, 14, 16] and their corresponding natural frequencies [16–18]. In all analyses, the Young's modulus, shear modulus and Poisson's ratio were assumed to be those of Al 7075-T6.

A smooth curve representing the distribution of cross-sectional properties can be formed from the reference distributions. The coefficients of these curves can then be tuned to give expected natural frequencies that match typical values. The second moments of area of the wing, I_{wing}, were assumed to follow an exponential relationship:

$$I_{\text{wing}} = a_1 e^{a_2 \eta} + a_3 \tag{1}$$

where a_1, a_2, and a_3 are unknown coefficients. In order to reduce the number of coefficients required required for tuning, the in-plane and out-of-plane second moments of area were assumed to be related to each other by a gain factor. The stiffness properties of the fuselage were assumed to follow a Gaussian distribution with other properties also related by a gain factor. The second moment of area of the fuselage, I_{fuselage}, is given by:

$$I_{\text{fuselage}} = b_1 e^{-\left(\frac{x-b_2}{b_3}\right)^2} + b_4 \tag{2}$$

where b_1 through b_4 are unknown coefficients that are tuned such that the fuselage natural frequencies match expected values.

It is common industrial practice to allow relative roll and relative yaw between the wings and the fuselage. Thus, the junction between the wings and fuselage was modelled using a rigid connection that was fixed in all translational directions and in the pitch-rotation direction, and a spring element (CELAS1 in *NASTRAN*) in the roll-rotation and yaw-rotation directions.

Different levels of flexibility were included in the model in order to observe the contribution that the flexibility of each part has on the overall response. The seven configurations are as follows:

1) Fully rigid airframe;
2) Fully flexible airframe;
3) Only flexible wings;
4) Only flexible fuselage;
5) Only flexible wings and fuselage;
6) Only flexible empennage; and
7) Only flexible wing/fuselage junction.

E. Landing Gear Attachment

The way in which the LG interfaces with the stick model can have an effect on the forces developed at the interface. The stick model represents the attachment using a single rigid element attaching the LG to the nearest node on the stick model, as seen in Fig. 2a. Cumnuantip and Krüger have shown that the way in which this interface is modelled, such as by using RBE3 elements in *NASTRAN* to attach the LG to multiple nodes, can have an effect on the loads developed [13]. However, as the purpose of this study is to compare the loads developed between various levels of airframe flexibility, a single rigid attachment was deemed sufficient and a study of the attachment is out of scope.

IV. *MSC Adams* Model

A. Model Setup

MSC Adams was used as the dynamic multi-body simulation platform. This allows simulation of flexible bodies by importing a modal neutral file (MNF) that is generated in *NASTRAN*, for simulating tires using *Adams Tire*, and for performing co-simulation between *MSC Adams* and *Simulink* to program the force model for the shock-strut. The airframe MNF file was imported and the LG was attached to the structure using a fixed constraint. The LG geometry was based on similarly-classed aircraft. A Fiala tire model was used in *Adams Tire*, with the tire geometry and properties based on those for a Boeing 737 [19]. The forces developed in the shock-strut are given by an oleo-pneumatic model, which is a simple force model that has been employed in literature for early investigations [13]. The air-spring force, F_s, is calculated from the expression governing polytropic gas expansion for air:

$$F_s = F_0 \left(1 - \frac{s}{s_t}\right)^{\gamma_{\text{air}}} \tag{3}$$

where s is the stroke distance, F_0 the preload force, γ_{air} the heat capacity ratio for air, and s_t is the total stroke length that is fixed by geometry. The damping force, F_d, is calculated as hydraulic damping through an orifice:

$$F_d = C_0 \text{sign}(\dot{s})\dot{s}^2 \tag{4}$$

where C_0 is the damping coefficient. The force model was programmed in to a *Simulink* model and run using the *MATLAB* co-simulation capability. *MSC Adams* outputs the stroke position and stroke velocity of the nose landing gear (NLG) and both main landing gear (MLG) to *Simulink*, which then calculates the force in each shock-strut and returns the value to *MSC Adams* to perform the integration for the time-step of the dynamic system; this block diagram is shown in Fig. 3.

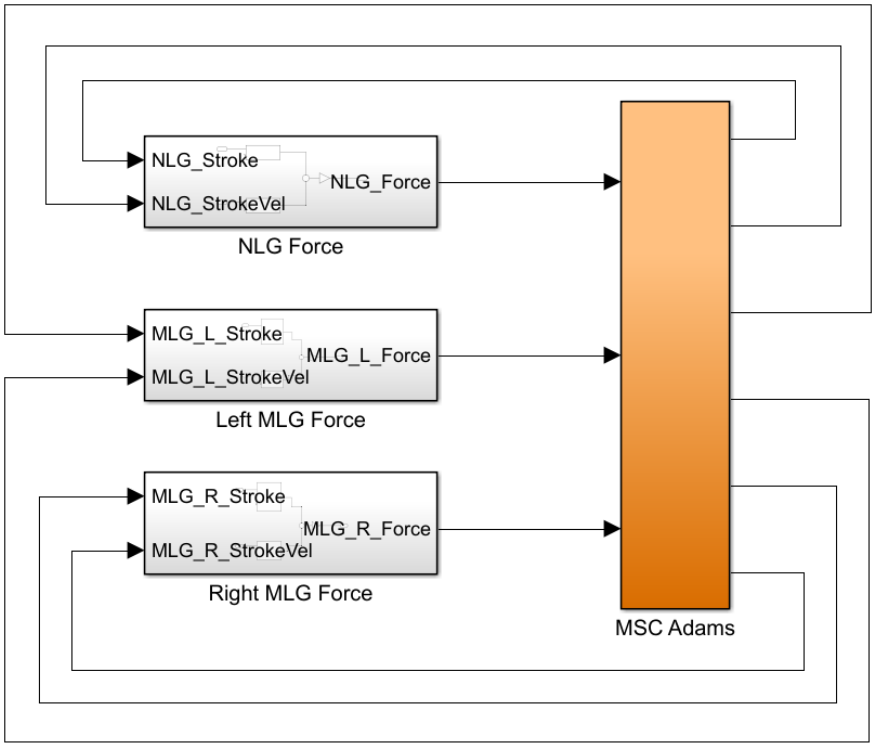

Fig. 3 *Simulink* block diagram.

B. Landing Cases

Three different scenarios were simulated: 3-point landing, tail-down landing, and asymmetrical landing (simulated crosswind). In all cases, initial contact with the runway occurs with a ground-relative forward velocity of 150 kts [77.1

m/s] and vertical descent velocity of 10 ft/s [3.0 m/s]. The initial conditions are summarized in Table 1. All simulations were performed to observe the open-loop response, meaning that no controls or brakes were used for the duration of the simulation.

Table 1 Initial aircraft body velocities and attitude.

	x-velocity		y-velocity		z-velocity		θ	ϕ	ψ
	[ft/s]	[m/s]	[ft/s]	[m/s]	[ft/s]	[m/s]	[deg]	[deg]	[deg]
Case 1	253	77.1	0	0	10.0	3.05	0	0	0
Case 2	240	73.3	0	0	52.5	16.0	10	0	0
Case 3	239	72.7	27.5	8.4	54.4	16.6	10	5	-7.5

V. Results and Discussion

Analyses were conducted to investigate the effect of the peak loads and loading regime between different airframe models.

A. Case 1: 3-Point Landing

For a symmetrical 3-point landing, the inclusion of wing flexibility results in a reduction of the peak loads, as shown in Fig. 4. A further reduction in the initial peak load is achieved by including a flexible fuselage. For a rigid aircraft and one with a flexible fuselage, there is a secondary peak load that is higher than the initial load; this behaviour is a remnant of the shock-strut force model as the initial peak is primarily due to the damping and the secondary peak due to air-spring compression. When all flexibility effects are considered, the peak force for the fully-flexible model is over 30% less than the peak for the rigid model. Further, the loading regime changes as there is not a secondary peak and there are higher-frequency vibrations.

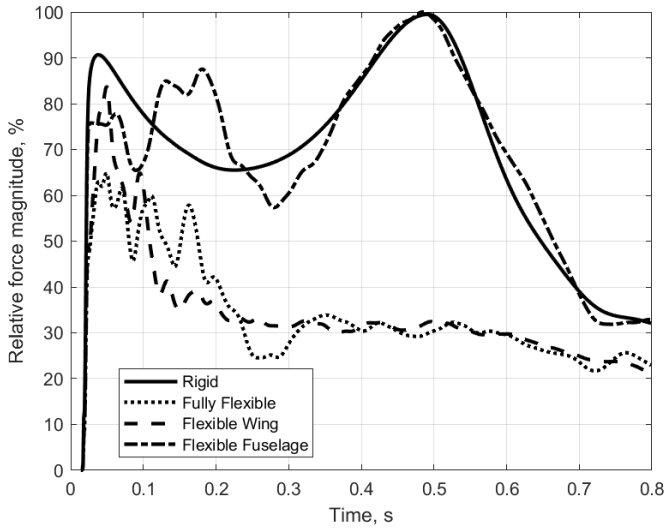

Fig. 4 Force magnitude normalized relative to the maximum observed force at the MLG attachment to the wing for Case 1.

In the symmetric landing case, there was a negligible effect on the structural dynamics that resulted from the inclusion of a flexible wing-fuselage junction and from flexibility of the empennage. As seen in Fig. 5, there is less than a 0.15% change in the force magnitude from the rigid model when considering the flexibility of these components. As the wing-fuselage junction permits movement out of the aircraft's xz-plane and a symmetric landing is symmetric about this plane, the additional degrees of freedom introduced would not be excited. Therefore, it was expected that the

flexible wing-fuselage junction has a negligible effect for a symmetric landing. Further, as the empennage mass is small compared to the mass of the aircraft and it has natural frequencies higher than those of the rest of the aircraft, it was expected that the empennage flexibility has a negligible effect on the loads for a symmetric landing.

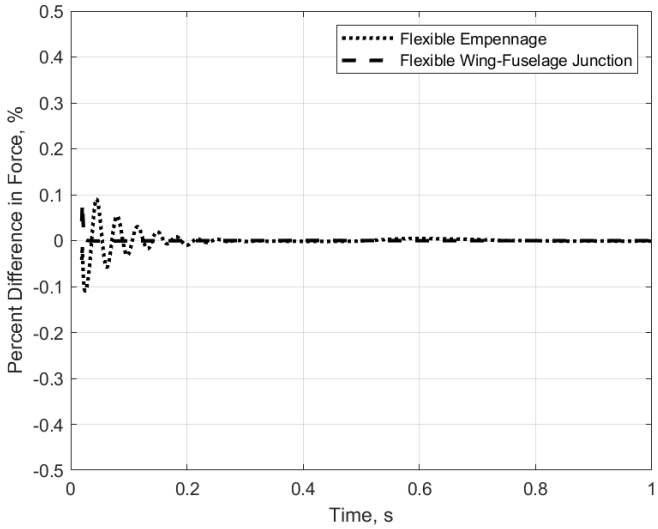

Fig. 5 Percent difference in MLG force magnitude versus rigid airframe model.

B. Case 2: 2-Point Landing

Similar observations of the loading were made for the symmetric tail-down landing as previously made for the 3-point landing. Additionally, it was observed that the additional torsional degrees of freedom introduced by flexibility of the wing changed the overall open-loop response of the aircraft. As seen in Table 2, the time for the NLG to contact the runway after initial contact by the MLG is reduced, and this reduction is mainly a result of the flexibility of the wing. When the MLG contacts the ground, there is a drag force that results in torsion of the wing. As a result, the contact point with the ground shifts further aft, which increases the nose-down pitching moment and thus alters the overall dynamics of the aircraft.

Table 2 Time of NLG contact after initial MLG impact for Case 2.

Model Used	Time Delta (s)
Fully Rigid Airframe	3.05
Flexible Wings Only	1.85
Flexible Fuselage Only	2.96
Fully Flexible Airframe	1.84

C. Case 3: Simulated Crosswind Landing

A crosswind landing is an asymmetric case in which one MLG contacts the runway before the other and introduces a side force on the LG. In this scenario, the port-side LG contacts the runway before the starboard-side, as seen in Fig. 6. As a result of the airframe flexibility effects, the peak moments at the MLG attachment to the wing are increased and there are higher-frequency loads that are introduced. Further, the time of contact of the second MLG for the flexible airframe model occurs later than the rigid model.

As this landing case is no longer symmetric about the aircraft's xz-plane, the effect of the flexible wing-fuselage junction becomes apparent. As seen in Fig. 7, the time of load rise is sooner, the initial peak load is higher, and the secondary peak load is lower when compared to the rigid airframe model. Also apparent in the figure is that the

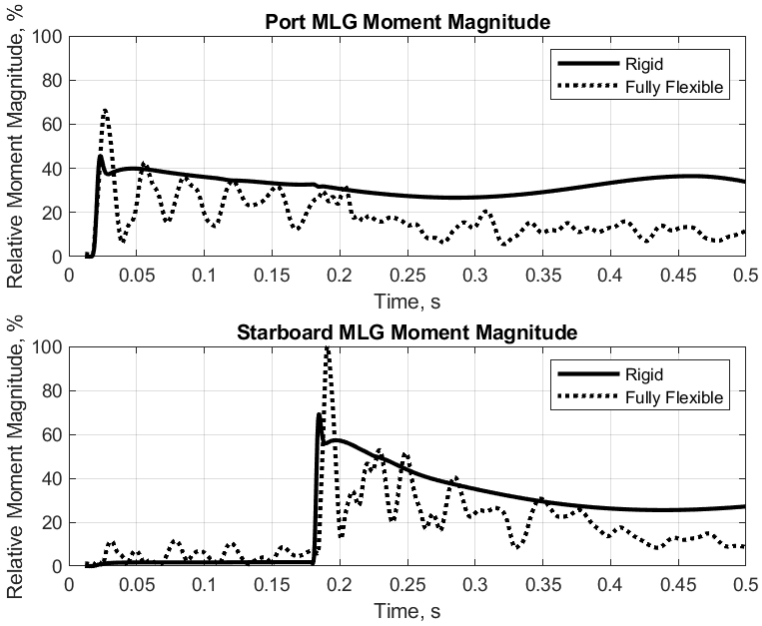

Fig. 6 Moment magnitude at the MLG attachment to the wing normalized with respect to the maximum moment at both MLG in Case 3.

inclusion of empennage flexibility has a noticeable effect on loading where both the primary and secondary peak loads are reduced when compared to the rigid airframe.

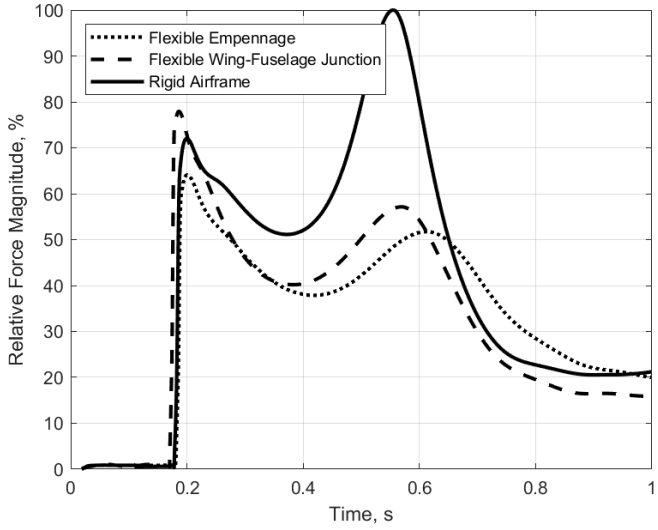

Fig. 7 Force magnitude at starboard MLG normalized relative to the maximum starboard MLG force in Case 3.

The inclusion of the airframe flexibility effects alters the peak loads, loading regime and overall response of the system. In general for this investigation, airframe flexibility effects resulted in a decrease in the peak forces but an increase in the peak moments at the connection between the LG and the wing when compared to a rigid aircraft model. Further, the vibrations of the structure results in higher-frequency loading. These differences change the way in which the components are loaded and will have consequences for structural optimization and predicted fatigue of the structure.

VI. Conclusion

A reduced FEM stick model of a generic regional jet was created via a novel approach and subsequently used in dynamic landing simulations to investigate the effects of airframe flexibility on landing loads and the loading regime. The following conclusions can be formed from this work:

1) In general, a reduction in the initial peak force but an increase in the initial peak moment at the attachment of the MLG to the wing was observed by including airframe flexibility effects.
2) The inclusion of airframe flexibility effects altered the loading regime by introducing higher-frequency loading.
3) Allowing relative yaw and relative roll between the fuselage and wings (flexible wing-fuselage junction) has no appreciable effect in symmetric landing conditions but alters the loads experienced in asymmetric landings. Therefore, it is necessary to include a flexible wing-fuselage junction.
4) The inclusion of empennage flexibility in a symmetric landing has a negligible effect on the peak loads but introduces higher-frequency vibrations that are small in comparison to the overall loads. The inclusion of empennage flexibility alters the loads experienced in asymmetric landings. Therefore, it is necessary to include empennage flexibility effects.

References

[1] Cook, F. E., and Milwitzky, B., "Effect of Interaction of Landing-Gear Behavior and Dynamic Loads in a Flexible Airplane Structure," techreport NACA-TR-1278, National Advisory Commitee for Aeronautics, Jan. 1956.

[2] Krüger, W., Besselink, I., Cowling, D., Doan, D., Kortüm, W., and Krabacher, W., "Aircraft Landing Gear Dynamics: Simulation and Control," *Vehicle System Dynamics*, Vol. 28, No. 2-3, 1997, pp. 119–158. doi:10.1080/00423119708969352.

[3] Pritchard, J., "Overview of Landing Gear Dynamics," *Journal of Aircraft*, Vol. 38, No. 1, 2001, pp. 130–137. doi:10.2514/2.2744.

[4] Brutto, D. L., Mastroddi, F., and D'Errioo, V., "Ground loads calculation of an aircraft flexible model," *MSC. ADAMS European Users Conference*, 2002.

[5] Khapane, P. D., "Simulation of asymmetric landing and typical ground maneuvers for large transport aircraft," *Aerospace Science and Technology*, Vol. 7, No. 8, 2003, pp. 611–619. doi:10.1016/s1270-9638(03)00066-x.

[6] Krüger, W., "A multi-body approach for modelling manoeuvring aeroelastic aircraft during preliminary design," *Proceedings of the Institution of Mechanical Engineers, Part G: Journal of Aerospace Engineering*, Vol. 222, SAGE Publications, 2008, pp. 887–894. doi:10.1243/09544100jaero264.

[7] Khapane, P. D., "Simulation of landing gear dynamics using flexible multi-body methods," *25th International Congress of the Aeronautical Sciences*, Vol. 6, Hamburg, Germany, 2006, pp. 3698 – 3707. Computer aided engineering tools;Flexible multi bodies;Gear dynamics;Gear walk;German aerospace centers;MBS Simulation;Product development cycle;Shimmy;.

[8] Nguyen, P., Mak, S., and Panza, J., "Simulation of Landing Events for an Unconventional UAV Landing Gear System Using Transient Dynamics Approach," *47th AIAA/ASME/ASCE/AHS/ASC Structures, Structural Dynamics, and Materials Conference*, American Institute of Aeronautics and Astronautics, 2006. doi:10.2514/6.2006-1762.

[9] Leo, R. D., Fenza, A. D., Barile, M., and Lecce, L., "Drop Test Simulation for An Aircraft Landing Gear Via Multi-Body Approach," *Archive of Mechanical Engineering*, Vol. 61, No. 2, 2014, pp. 287–304. doi:10.2478/meceng-2014-0017.

[10] Sartor, P., Schmidt, R., Becker, W., Worden, K., Bond, D., and Staszewski, W., "Conceptual Design of a Hard Landing Indication System Using a Flight Parameter Sensor Simulation Model," *27th International Congress of the Aeronauical Sciences*, 2010.

[11] Lee, K. B., Jeong, S. H., Cho, J. Y., Kim, J. H., and Park, C. Y., "Hard-landing Simulation by a Hierarchical Aircraft Landing Model and an Extended Inertia Relief Technique," *International Journal of Aeronautical and Space Sciences*, Vol. 16, No. 3, 2015, pp. 394–406. doi:10.5139/ijass.2015.16.3.394.

[12] Bronstein, M., Feldman, E., Vescovini, R., and Bisagni, C., "Assessment of dynamic effects on aircraft design loads: The landing impact case," *Progress in Aerospace Sciences*, Vol. 78, 2015, pp. 131–139. doi:10.1016/j.paerosci.2015.06.003.

[13] S. Cumnuantip, and W.R. Krüger, "Assessment of Dynamic Landing Loads by a Hybrid Multibody / Full Finite Element Simulation Approach," *German Aerospace Congress 2018*, Deutsche Gesellschaft für Luft- und Raumfahrt - Lilienthal-Oberth e.V., 2018. doi:10.25967/480116.

[14] Elsayed, M. S. A., Sedaghati, R., and Abdo, M., "Accurate Stick Model Development for Static Analysis of Complex Aircraft Wing-Box Structures," *AIAA Journal*, Vol. 47, No. 9, 2009, pp. 2063–2075. doi:10.2514/1.38447.

[15] Roskam, J., *Airplane Design - Part V: Component Weight Estimation*, Design, Analysis and Research Corporation, 1999.

[16] Cirillo, R., "Detailed and condensed finite element models for dynamic analysis of a business jet aircraft," Ph.D. thesis, Politecnico Di Milano, 2011.

[17] Castellani, M., Cooper, J. E., and Lemmens, Y., "Flight Loads Prediction of High Aspect Ratio Wing Aircraft Using Multibody Dynamics," *International Journal of Aerospace Engineering*, Vol. 2016, 2016, pp. 1–13. doi:10.1155/2016/4805817.

[18] Thomas, P. V., ElSayed, M. S. A., and Walch, D., "Review of Model Order Reduction Methods and Their Applications in Aeroelasticity Loads Analysis for Design Optimization of Complex Airframes," *Journal of Aerospace Engineering*, Vol. 32, No. 2, 2019, p. 04018156. doi:10.1061/(asce)as.1943-5525.0000972.

[19] Daugherty, R. H., "A Study of the Mechanical Properties of Modern Radial Aircraft Tires," techreport NASA/TM-2003-212415, NASA Langley Research Center, Hampton, Virginia, May 2003.